Available online at www.sciencedirect.com
SCIENCE DIRECT®
International Journal of Thermal Sciences 45 (2006) 739–751
International Journal of Thermal Sciences
www.elsevier.com/locate/ijts

Flow boiling of pure fluids: local heat transfer and flow pattern modeling through artificial neural networks

G. Scalabrin *, M. Condosta, P. Marchi

Dipartimento di Fisica Tecnica, Università di Padova, via Venezia 1, I-35131 Padova, Italy

Received 28 June 2005; received in revised form 5 August 2005; accepted 16 September 2005
Available online 22 December 2005

Abstract

A new modeling technique based on neural networks as a universal function approximator has been applied to study the local representation of flow boiling heat transfer at varying fluid dynamics conditions along the tube, i.e., moving through different flow pattern regions. After subdivision of the experimental data into subsets homogeneous for flow conditions, specific heat transfer equations have been heuristically got. Such specific equations have been validated and compared with the global MLFN heat transfer coefficient representation for the same target fluid as from a former work. The study has been extended to four fluids for which suitable data were available from the literature. The representation accuracies of the specialized heat transfer models are very high, even if such a method is not in general suggested due to the greater complication for both the equations development and for their practical use. It was furthermore shown that a global high accuracy flow boiling heat transfer equation can be developed also without any relation with local fluid dynamics conditions. A new modeling technique has been furthermore proposed for the fluid dynamics conditions along the tube. The linking of the picture of the actual flow condition directly with a conventional continuous real number, the so-called SF factor, allows to convert the flow condition into a numerical variable which can be turned into a continuous fluid specific function through a further MLFN technique. Limitedly to the few available literature SF data the method presents high performance and coherence for the whole SF surface. The present SF MLFN equation and the more advanced literature flow pattern model get comparable results, in spite of the limited data base. It is also shown that a flow boiling heat transfer model is not intrinsically flow pattern dependent, because a flow condition representation is never required for a global heuristic heat transfer coefficient modeling.

Keywords: Flow boiling; Flow pattern; Heat transfer modeling; Inside smooth tubes; Neural networks; Pure fluids

1. Introduction

The representation of the flow boiling heat transfer of a pure fluid inside a tube is a difficult task which is increased in the case of a horizontal arrangement as a consequence of the action of gravity tending to separate the liquid and the vapor phases at each section. The fluid dynamics conditions along the tube progressively change in a macroscopic way as the vapor fraction increases and the heat transfer dynamics follow this development with a parallel but distinct evolution. The tendency to the phase stratification caused by the horizontal position and the lower density of vapor lead to a rapid increase of the vapor to liquid relative velocity causing a vapor to liquid share stress with a rather complex fluid dynamics situation which is very difficult to represent.

Considering in general the literature models for flow boiling one can see that the models have been in any case developed using some kind of empirical approach. In fact a preliminary tentative model is at first assumed and it has to undergo successive modifications to correct discrepancies with respect to experimental data using a 'trial-and-error' approach. The analytical terms of these modifications are substantially empirical and have been historically developed through a long series of enhancements. For a further improvement new series of experimental data are always required to study in more detail the unreliable behaviors of the models leading them to be substantially tuned on the data, but through a sort of conflictual relationship with them. These models aim at predicting the heat

* Corresponding author. Tel.: +39 049 8276875; fax: +39 049 8276896.
E-mail address: gscala@unipd.it (G. Scalabrin).

1290-0729/$ – see front matter
doi:10.1016/j.ijthermalsci.2005.09.010

Nomenclature

AAD	average absolute deviation	
Bias	bias	
d	diameter	m
f_{ob}	objective function	
$f(x)$	transfer function	
H_i	output layer value	
I	number of neurons in input layer	
J	number of neurons in hidden layer	
K	number of neurons in output layer	
$\dot{m}$	mass flow rate	$\mathrm{kg\,m^{-2}\,s^{-1}}$
NPT	number of points	
$\dot{q}$	heat flux	$\mathrm{W\,m^{-2}}$
SF	Strömungform = form of the flow	
S_i	output layer value	
T	temperature	K
U_i	input layer value	
V_i	physical input	
W_k	physical output	
x	generic variable	
$\dot{x}$	vapor quality	

Greek symbols

α	heat transfer coefficient	$\mathrm{W\,m^{-2}\,K^{-1}}$
β	span coefficient	
γ	steepness coefficient	
Δ	error deviation	

Superscript

calc	calculated
exp	experimental

Subscript

b	boundary
c	critical
i	target fluid
r	reduced

transfer data, but their functional forms are in the meantime always conditioned by them.

Furthermore, it cannot be assured that an empirical preliminary tentative model is in general suitable to 'converge', through a series of 'trial-and-error' successive modifications, to a reliable formulation able to accurately describe a heat transfer phenomenon. Due either to the preliminary model architecture or to the successive modifications strategy or to both of them, the method on the whole could not be able to 'converge' at all, also independently from the efforts spent for the study.

Sometimes it also happens that, after the development of an innovative model for flow boiling [1,2], claiming to be predictive, i.e., suitable for a large number of fluids, right after its functional form is again arranged for turning it to represent the inexplicable heat transfer behavior of a further fluid [3]. In this case the coherence is evidently lost.

One could wonder whether a possibility exists to exit from this circle assigning to the experimental data the leading role, because they are ruling in any modeling technique. This consequently means to move to totally heuristic modeling techniques leaving out any 'theoretical foundation', similarly to what has been very effectively done in recent times for the thermodynamic [4] and transport properties [5,6] domains.

In a previous work [7] the heuristic modeling of the heat transfer coefficient for flow boiling inside a horizontal tube has been solved with success through the use of neural networks as general function approximators. It was shown that an individual heat transfer equation, with the controlling physical variables as independent variables, can be directly drawn from experimental data and that this can cover the whole variables range. The prediction accuracy limit of the new method is substantially determinated by the data uncertainty, if they are distributed with sufficient regularity. This technique allows to get a very precise form of the heat transfer coefficient expressed as a fluid specific continuous function $\alpha_i = \alpha_i(T_r, \dot{m}, \dot{q}, \dot{x}, d)$ or, alternatively, $\alpha_i = \alpha_i(T_r, \dot{m}, \dot{q}, \dot{x})$ in the case data are not present at different diameters.

This new modeling opportunity suggests now to reconsider from the beginning the problem of the variation of the heat transfer coefficient along the tube during the progression of the vapor generation applying these same techniques for the analysis of specific aspects of the phenomena. It could be in particular interesting to draw heat transfer functions at different flow pattern conditions from homogeneous subsets of the data and to compare these specific functions with the global function.

Furthermore, being these methods totally heuristic, it could be possible to analyze the relations, if any, between the flow pattern and the heat transfer behavior, looking at a possible local representation of the heat transfer more detailed and accurate with respect to the global one.

The goal of the present work is then to study the local representation of the flow boiling heat transfer at varying fluid dynamics conditions along the tube, i.e., moving through different regions of flow conditions.

2. Neural networks

In order to overcome the fitting problem of the heat transfer coefficient function $\alpha(T_r, \dot{m}, \dot{q}, d, \dot{x})$ a powerful function approximator, with an *a priori* known functional form, is proposed to be introduced. The vector of parameters $\bar{w}$ for the function approximator has then to be regressed through a minimization technique and for that an objective function has to be minimized. The objective function f_{ob} here taken is:

$$f_{ob} = \frac{1}{NPT}\sum_{i=1}^{NPT}\left(\frac{\alpha_i^{calc} - \alpha_i^{exp}}{\alpha_i^{exp}}\right)^2 \tag{1}$$

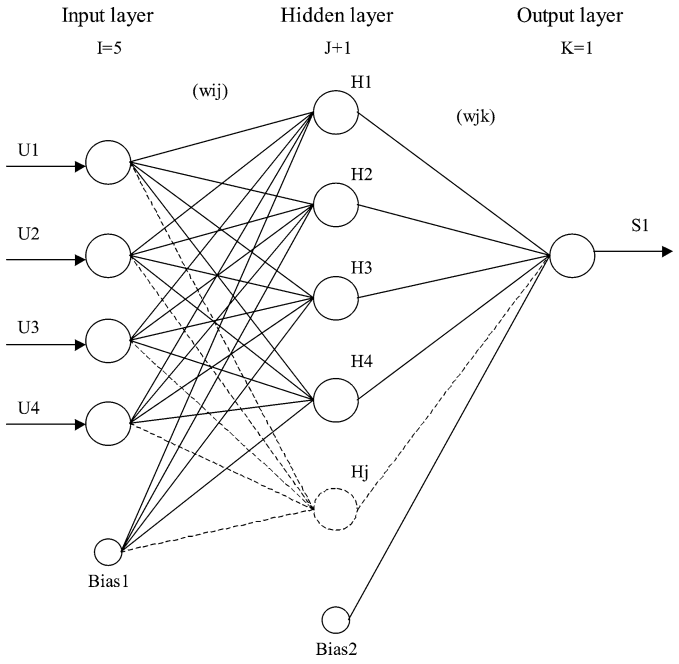

Fig. 1. Schematic representation of the multilayer feedforward neural network (MLFN) for the present study.

where NPT is the number of experimental points, α_i^{calc} is the heat transfer coefficient calculated value, α_i^{exp} is the heat transfer coefficient experimental value.

Among the more powerful function approximators with an a priori known functional form, there is the *multilayer feedforward neural network* (MLFN), which has been formerly applied for transport properties modeling by the same authors [6]. The structure of this function approximator, chosen for the present regression, is schematically drawn in Fig. 1.

In this architecture, there are several neuron layers (*multilayer*) and the information goes in only one direction, from input to output (*feedforward*), i.e., from left to right in Fig. 1. The *I-1* inputs U_i enter the *I-1* neurons of the input layer. The inputs U_i represent the independent variables of the problem. The transfer function $f(x)$ converts the inputs to outputs in the neuron and in the present work it has a sigmoid form:

$$f(x) = \gamma \frac{1}{1 + e^{-2\beta x}} \tag{2}$$

The analytical form of the present MLFN is:

$$H_j = f\left(\sum_{i=1}^{I} w_{ij} U_i\right) \tag{3}$$

$$U_I = Bias\ 1 \tag{4}$$

$$S_k = f\left(\sum_{j=1}^{J+I} w_{jk} H_j\right) \tag{5}$$

$$H_{J+I} = Bias\ 2 \tag{6}$$

with $1 \leqslant i \leqslant I-1$, $1 \leqslant j \leqslant J$, $1 \leqslant k \leqslant K$, where the function f in Eqs. (3) and (5) is Eq. (2).

In our case the inputs U_1, U_2, U_3, U_4, and U_5 refer respectively to T_r, $\dot{m}$, $\dot{q}$, $\dot{x}$, and d, the output S_1 is the heat transfer coefficient function $\alpha(T_r, \dot{m}, \dot{q}, \dot{x}, d)$, whereas w_{ij} and w_{jk} are the parameters to regress. The number of neurons in the hidden layer J can be varied searching for the lowest value of the minimized f_{ob} function.

For more details about the characteristics of the MLFN application reference is also made to a previous heat transfer modeling for heating and cooling of supercritical carbon dioxide [8,9].

3. Heat transfer correlations specific for a single flow condition range

As discussed in the introduction an innovative technique, based on MLFN, has been proposed in a former work [7] to heuristically draw, directly from experimental data, an analytical formulation of the heat transfer coefficient surface of a target fluid for flow boiling inside horizontal tubes. The results obtained in that work allow to represent such heat transfer surface through a unique functional form whose parameters are evidently fluid dependent. One of the most important results obtained from the proposed modeling technique is the capability to represent with a single function the heat transfer surface in the whole ranges of the independent physical variables controlling the heat transfer coefficient.

Through this procedure the functional form of the heat transfer coefficient can then be expressed as a fluid specific continuous function:

$$\alpha_i = \alpha_i(T_r, \dot{m}, \dot{q}, \dot{x}, d) \tag{7}$$

or, alternatively:

$$\alpha_i = \alpha_i(T_r, \dot{m}, \dot{q}, \dot{x}) \tag{8}$$

in the case data are not present at different diameters.

The proposed method can be evidently applied to any set of heat transfer data, either in the whole range of the independent physical variables or in a subset of them including all the points pertaining to one of the homogeneous fluid dynamics conditions developed along the tube as the vapor quality grows. It could be interesting to get heat transfer equations for subsets of data pertaining to homogeneous fluid dynamics conditions and to compare such equations with the global one representing the whole data population. This is in other words an analysis of the heat transfer surface characterization inside predefined flow conditions ranges and of the possible relations between a heat transfer surface and the fluid dynamics conditions. In order to develop such a study an accurate subdivision of the heat transfer data population according to the flow condition for each target fluid has to be preliminarily produced.

The local fluid dynamics condition can be known either by experimental observation or by a flow pattern predicting model. In the first case the data reliability is certainly better than in the second case where the inaccuracy of the model can be determinant for the composition of the data subsets and then for the analysis.

Unluckily, the literature data sets reporting such experimental observations are very few and in most of the cases it is necessary to resort to flow pattern models to assign a flow condition

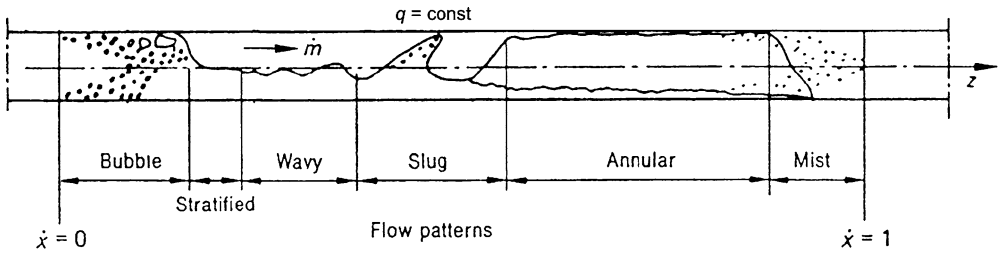

Fig. 2. Schematic representation of the flow boiling fluid dynamics conditions along a horizontal tube for constant $\dot{q}$.

to each point losing then the experimental reliability. In the present study the directly accessible experimental observations will be preferred whenever available and the characterization from flow pattern models will be used as an alternative. The recent and updated flow pattern model from Thome et al. [10] is assumed for the study. Comparisons between results obtained in the two modes will be also discussed.

For each of the fluid considered in this work an overall heat transfer equation has been developed in a former work [7], to which reference is made in the discussion.

4. Development of fluid and flow condition specific heat transfer correlations

Four pure fluids disposing of a sufficient number of experimental points have been considered. Unfortunately this heat transfer scientific domain suffers from a systematic lack of published experimental measurements, which on the contrary are absolutely indispensable in particular to analyze this complex subject. The available data sets have been divided into two subsections: those with the simultaneous experimental observation of the local fluid dynamics condition and those lacking in it. The two cases are separately dealt with in the following paragraphs. In the present study only experimental sources with a sufficiently large number of points are considered to allow reliable regressions and validations of the developed equations.

In the present work the error deviation (Δ), the average absolute deviation (AAD) and the bias (Bias) are evaluated as:

$$(\Delta\%)_i = \frac{\alpha_i^{\text{calc}} - \alpha_i^{\text{exp}}}{\alpha_i^{\text{exp}}} \times 100$$

$$AAD\% = \frac{1}{NPT}\sum_{i=1}^{NPT} |\Delta\%|_i$$

$$Bias\% = \frac{1}{NPT}\sum_{i=1}^{NPT} (\Delta\%)_i \tag{9}$$

The numerical elements of the obtained MLFN heat transfer equations are not reported in this work for sake of brevity and also because the main aim is to present and discuss fundamental aspects of a new modeling procedure, instead of going into details of this or that specialized equation.

4.1. Experimental flow characterization

Only for the fluid R12 a literature source [11] was found reporting the heat transfer data together with the experimental observation of the local fluid dynamics condition. This data source divides the points into several subsets characterized by the fluid dynamics conditions progressively encountered.

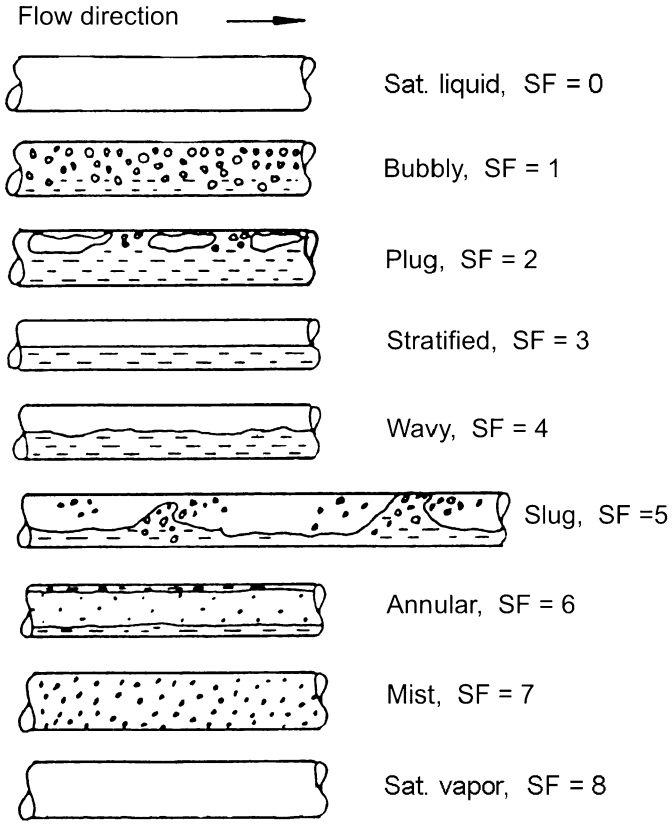

Fig. 3. Basic fluid dynamics conditions with the value of the corresponding SF assigned value.

Each of these subsets is marked out by a conventional figure, ranging from 0 to 8, that is indicated as *SF* (Strömungform = form of the flow). Basing on a picture of the fluid dynamics evolution of the boiling inside the tube from the saturated liquid condition at the entrance to the full vapor at saturated conditions at the exit, integer SF values are assigned to each typical and completely identified fluid dynamics situation, as for instance stratified, wavy, annular, etc. A non-integer SF number is assigned to intermediate flow conditions. In Fig. 2 the homogeneous fluid dynamics conditions developed along the tube as the vapor quality grows are shown and in Fig. 3 the completely identified conditions corresponding to integer SF values are reported.

This format allows to continuously evaluate the flow condition at each section according to the experimenter observations and to represent it through a conventional number as SF.

This procedure is very interesting because it allows to objectively convert the present experimental observation of the flow condition, simultaneous with the heat transfer coefficient measurement, into a measurable conventional quantity whose range could be suitably defined. In the case such a method would be generally adopted for this experimental domain, it would be possible to 'quantify' the flow evaluation and to transform the conventional observations of the flow from qualitative and in a discrete form into quantitative and continuous.

For the case of R12 the Schmidt data [11] are distributed from the bubbly to the mist condition. The SF values given by the author lie in the 0 to 9 range but Fig. 6 is not associated to a defined condition. To uniform the SF values in a regular range the values greater than 7 have been decreased of a unity converting the original 0 to 9 range into the equivalent 0 to 8 range of the present conventional scale. In order to subdivide the data into few and rather homogeneous flow conditions, also considering the limited amount of data, three SF ranges have been selected. A first range has been identified including the stratified-like conditions with SF in the range 2.5 to 4.5. A second range was chosen for the slug-like conditions, characterized by an intermittent wetting of the tube upper wall, with a range from 4.5 to 5.5. The third range includes the annular-like conditions in the range higher than 5.5. Few points falling in the bubbly condition were omitted from the study because they were too few to sufficiently describe that region.

The points incidentally lying on the range boundary are assumed to belong to both the preceding and the following subset to wide the number of data in each subset and to better smooth the local heat transfer equations in the correspondence of the boundaries.

The whole data base has then been divided into three parts: a stratified + wavy, a slug, and an annular + mist subset. For each of these subsets a MLFN heat transfer equation has been obtained and the corresponding validations are reported in Table 1. For sake of precision the overall number of points does not correspond with the NPT sum of the three cases because, as previously explained, the points exactly at the SF boundary range values were considered both in the preceding and in the following subset. Since no other source is available for this fluid the MLFN equations were trained on all the presently available data with the consequence that the validation results have to be considered as residual errors of the obtained surfaces.

The behaviors of the three MLFN heat transfer equations for the flow condition subsets are comparable each other both in the values of the residual deviation (AAD) and in the shifting (Bias). In any case the obtained results are also comparable with the current values of experimental uncertainties for flow boiling. The performance of the overall MLFN equation [7] is always worse both for the residual errors and for the shifting. The experimental quality of these data is considered as rather questionable from the point of view of both their uncertainty and of their experimental subdivision according to the flow conditions.

Anyway, a defined trend can be recognized showing the local equations to perform always better than the global one. This can be explained considering the different functional dependences of the heat transfer coefficient on the independent physical variables for each of the three cases and the requirement for the overall equation to represent in a single functional dependence all the three surfaces. The processing of a reduced amount of data, locally contained and quite homogeneous from the functional dependence point of view, leads to a better fitting capability of the same modeling tool. Also the error noise and the uncertainties of the data play an evident role in decreasing the fitting accuracy when the data have to be processed all together. The representation of a global surface as the union of a number of component sub-surfaces is certainly an easier task for a function approximator.

4.2. Predictive flow characterization

Except for the former fluid R12 all the other available experimental sources for heat transfer do not report observations of the flow conditions simultaneous with the heat transfer measures. As a consequence, for all the following cases the heat transfer data will be divided into three subsets roughly homogeneous for flow conditions on the base of a flow pattern model that will be always assumed from Thome et al. [10]. As usual the literature is rather lacking of published data and for only the three fluids R11, R22, and R134a a sufficient base of data was made available.

4.2.1. Case of fluid R11

For R11 only the source of Chawla [12] was found and the model was trained uniquely on these points. The subdivision

Table 1
Heat transfer MLFN equations results for the R12 data, experimental flow subdivision

Ref.	*NPT*	Flow	T_r range	$\dot{m}$ range [kg m^{-2} s^{-1}]	$\dot{q}$ range [W m^{-2}]	$\dot{x}$ range	*d* [mm]	*AAD* %	*Bias* %	*AAD* %	*Bias* %
								Flow pattern specific equation		Overall equation [7]	
[11]	355	Stratified + Wavy	0.65–0.76	39–403	11–80200	0.07–0.83	14	13.12	−3.40	19.57	−4.37
[11]	227	Slug	0.65–0.76	39–406	16–80200	0.02–0.83	14	14.81	−3.59	21.82	−12.91
[11]	213	Annular + Mist	0.65–0.76	125–578	15–70900	0.05–0.84	14	10.18	−1.64	16.79	−6.31
	679	Overall	0.65–0.76	39–578	11–80200	0.02–0.84	14	12.66	−2.43	19.40	−6.68

Table 2
Heat transfer MLFN equations results for the R11 data, flow pattern model subdivision

Ref.	*NPT*	Flow	T_r range	$\dot{m}$ range [kg m^{-2} s^{-1}]	$\dot{q}$ range [W m^{-2}]	$\dot{x}$ range	*d* [mm]	*AAD* %	*Bias* %	*AAD* %	*Bias* %
								Flow pattern specific equation		Overall equation [7]	
[12]	608	Stratified + Wavy	0.58–0.62	12–163	350–2320	0.10–0.90	6–25	6.45	−0.70	7.03	−0.73

Table 3
Heat transfer MLFN equations results for the R22 data, flow pattern model subdivision

Ref.	*NPT*	Flow	T_r range	$\dot{m}$ range [kg m^{-2} s^{-1}]	$\dot{q}$ range [W m^{-2}]	$\dot{x}$ range	*d* [mm]	*AAD* %	*Bias* %	*AAD* %	*Bias* %
								Flow pattern specific equation		Overall equation [7]	
[13,14]	481	Slug	0.71–0.78	200–1064	4250–30000	0.01–0.39	7.7–10.7	5.22	−0.53	6.41	−0.74
[13,14]	530	Annular	0.71–0.78	150–852	4250–30000	0.32–0.94	7.7–10.7	3.23	−0.20	4.04	−0.49
[13]	407	Slug	0.71–0.78	240–1064	4250–30000	0.01–0.39	7.7	5.62	−0.55	7.03	−1.13
[13]	266	Annular	0.71–0.78	240–852	4250–30000	0.32–0.86	7.7	3.75	−0.15	4.20	0.65
[14]	74	Slug	0.78	200–300	10000–30000	0.17–0.38	10.7	3.00	−0.43	3.02	1.39
[14]	264	Annular	0.78	150–300	10000–30000	0.39–0.94	10.7	2.71	−0.25	3.88	−1.64
[13,14]	1011	Overall	0.71–0.78	150–1064	4250–30000	0.01–0.94	7.7–10.7	4.18	−0.36	5.17	−0.61
[13]	673	Overall	0.71–0.78	240–1064	4250–30000	0.01–0.86	7.7	3.41	−0.39	5.91	−0.43
[14]	338	Overall	0.78	150–300	10000–30000	0.17–0.94	10.7	2.77	−0.29	3.69	−0.98

into the flow regions resulted in a largely predominant stratified + wavy subset, while about one hundred points fall in the remainder regions. As a consequence only the data population of the larger subset is sufficient for a heuristic study. The case of the present fluid is the only one for which the heat transfer equation was got with also the functional dependence on the tube diameter thanks to this dependence in the available data. The results are presented in Table 2.

In the present case the performances of the flow pattern specific equation and of the overall one [7] are quite close one to the other with only a slightly better result for the first one; both present a very low bias value assuring that any systematic shifting is absent. It looks reasonable to suppose that the obtained prediction performances are quite close to the experimental quality of the data and that the reached limit is also the intrinsic limit of the data uncertainty; in fact these would be very good statistical figures for an experimental work.

4.2.2. Case of fluid R22

For the fluid R22 two reliable experimental sources were made available [13,14]. The data from Kim et al. [13] have been subdivided with the flow pattern model and two main subsets were identified in the regions of slug and annular flow, respectively. Similarly, the data from Lallemand et al. [14] have been subdivided into the same two flow conditions as before. For both the sources the data falling outside these subsets form groups of too few points, it is then not possible to process them for obtaining further equations.

The available data of the Kim et al. [13] and Lallemand et al. [14] sets for each flow condition were composed together to form the two data bases on which the trainings were performed. Two different heat transfer equations were then obtained for each of the two flow conditions and in this case the validation results of the equations are to be considered only as residual deviations. In Table 3 the obtained results are reported for both the flow pattern specific equations and for the overall one [7]. The first two lines of the table report the training results for each of the flow pattern specific equations, together with the comparison with the heat transfer equation for the whole flow pattern range [7]. In the following lines the validations of both the specific and overall equations with respect to the slug and annular subsets of each of the two sources are shown. Both the flow pattern specific equations produce very good results close one to the other in error deviations and in bias values. For each of the subsets their performance is slightly better than the overall equation, more likely due to the narrower region of the heat transfer surface to represent by the specific equations. In any case the differences between these representations are largely below the current experimental errors for heat transfer so that this kind of resolution is well sound for the trends.

The validation of the equations inside each single source subset shows a quite similar behavior also demonstrating that the two sources have high and comparable experimental qualities.

4.2.3. Case of fluid R134a

For the fluid R134a the experimental sources are limited to Kim et al. [13,15] and for this one the flow pattern model subdivision resulted in the two slug and annular subsets; a limited amount of points outside these ranges has been neglected. In Table 4 the final results are reported.

As verified for the former cases also here the performances are very high and the flow pattern specific equations are performing slightly better than the overall one. The behavior is

Table 4
Heat transfer MLFN equations results for the R134a data, flow pattern model subdivision

Ref.	*NPT*	Flow	T_r range	$\dot{m}$ range [kg m^{-2} s^{-1}]	$\dot{q}$ range [W m^{-2}]	$\dot{x}$ range	d [mm]	*AAD* %	*Bias* %	*AAD* %	*Bias* %
								Flow pattern specific equation		Overall equation [7]	
[13,15]	238	Slug	0.71–0.78	239–854	4220–30000	0.01–0.35	7.7	4.69	−0.43	5.83	−0.77
[13,15]	251	Annular	0.70–0.77	239–742	4200–30000	0.27–0.89	7.7	2.92	−0.22	3.80	−0.13
[13,15]	489	Overall	0.70–0.78	239–854	4200–30000	0.01–0.89	7.7	3.78	−0.32	4.79	−0.44

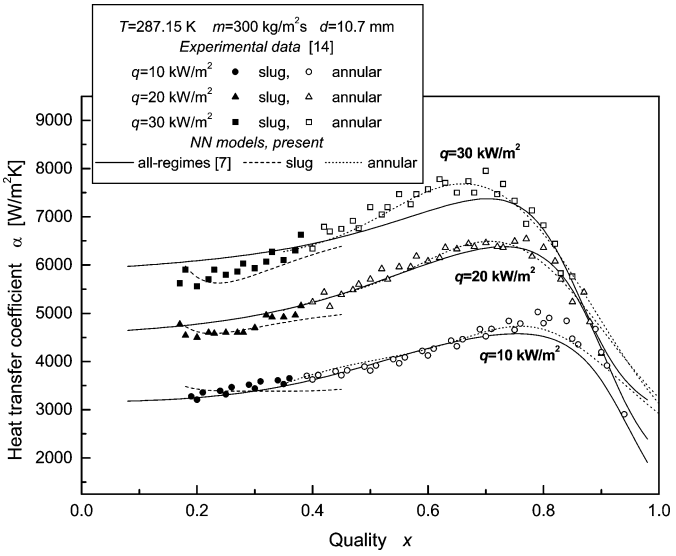

Fig. 4. Fluid R22: heat transfer coefficient α vs. vapor quality $\dot{x}$, parametric in heat flux $\dot{q}$ for assigned values of T, $\dot{m}$, d. Comparison among the predictions by the MLFN overall equation (continuous lines), the flow pattern specific equations (dotted and dashed lines), and experimental data [14].

absolutely coherent with the preceding ones and then very similar comments can be drawn. The results are considered as self explaining.

5. Effects of model specialization according to flow pattern

In the former section it has been shown that the division of the heat transfer data for a target fluid into subranges as much as possible homogeneous in fluid dynamics conditions allows to increase the accuracy of the obtained single flow pattern specific equations. As an example the case of fluid R22 is studied for this purpose and the effect of increasing the accuracy is shown in Fig. 4, where sections of the MLFN flow pattern specific and overall equations are plotted together with the experimental points used for training with respect to vapor quality $\dot{x}$, parametric in heat flux $\dot{q}$ for assigned values of T, $\dot{m}$, d. As discussed for the former Table 3 the data population resulted to be divided into two main subgroups pertaining to the slug and annular regimes.

Fig. 4 clearly shows the effect of the specialization of a MLFN according to a narrow range of fluid dynamics conditions. In fact the sections of the slug and annular equations follow quite finer the experimental points demonstrating to better adapt themselves to a more limited extent of a heat transfer surface, which is known through the experimental data. The continuous line representing the all-regimes equation is asked to follow at once all the data inevitably producing a compromise among their values. A perfect interpolation of the points is also hindered by the experimental error noise, even if in this case it is rather low.

The representation of Fig. 4 shows very clearly the significance and the effects of heuristically describing a heat transfer surface either by a single equation of by a number of more precise flow pattern specific equations, aiming, in the second case, at representing the whole surface through a sort of patchwork of local equations.

The results of the former study [7] had already shown that the heat transfer coefficient surface for flow boiling inside a horizontal tube can be represented through the present heuristic method in a single solution for the whole range of flow pattern conditions encountered along the tube. The present study looks at the analysis of local subsets of that overall problem aiming to verify some characteristics and advantages of the method. In general this second approach tends to highlight finer details of the same problem, basically pertaining anyway to the overall solution [7].

6. Modeling of flow pattern maps

Considering both the representation ease of the heat transfer coefficient surface as demonstrated in the preceding and the high effectiveness of the present heuristic method, one could wonder whether the same technique could be extended to analytically represent the flow pattern as a function of the controlling physical variables. Since the present aim is the set up of a new mathematical function including all the variables on which flow pattern depends, the first difficulty is posed by the numerical and continuous quantification of the local flowdynamic condition. It is evident that the flow conditions cannot be associated with a real physical variable and that such a representation has then necessarily to move to a conventional figure conveniently defined.

An advantage could be taken from the former discussion at Section 4.1 where the conventional *SF* (Strömungform = form of the flow) factor was considered [11]. The SF is a conventional non-integer number ranging from 0 to 8 which is directly associated with a defined flow-dynamic condition according to current experimental observations, see Figs. 2 and 3. Having preliminarily defined a conventional figurative representation of the flow condition evolution along the tube, as

for instance that of Fig. 2, and associating progressive integer values of SF to precise and characteristic flow conditions of that representation, see for example Fig. 3, the biunique correspondence between flow condition and SF value could be established. In this way a unique and fluid dynamically defined condition would correspond to a SF value and vice versa. Once the figurative evolution of the flow condition would be defined, Fig. 2, and the position on it of the fixed points would be chosen assigning to them progressive SF integer values, in an arbitrarily defined range and with progressive real SF values in between two integers, Fig. 3, the SF numerical value becomes a normalized representation of a defined local condition of flow. In this way in correspondence of a direct experimental observation of the flow condition a defined SF value is assigned by the experimenter performing for that condition a heat transfer coefficient measurement. The experimenter could simultaneously get two observations, the α value measurement and the SF value evaluation, giving raise to a coherent data base.

Through this procedure the very complex physical behavior of a local fluid dynamics condition remains unknown but that condition is biuniquely identified by the local SF value: the local picture of the flow condition substitutes the analysis of the local physical behavior.

The complicated and very cumbersome inside physical analysis of such phenomena, inevitably of limited precision, represents a distinct domain of study with which the present method does not interfere.

On the other hand, from the extensive literature about flow patterns the knowledge of the operative physical variables controlling these phenomena during flow boiling at saturation conditions is well consolidated: they are the reduced temperature T_r, the mass flow rate $\dot{m}$, the vapor quality $\dot{x}$, the inside diameter of the tube d and, only at certain conditions, the heat flux $\dot{q}$. For each combination of the values of these variables the flow condition is directly identified. Because we can now associate to a flow condition the corresponding value of SF we could combine the SF value with the corresponding values of the independent variables at the present condition.

Once a data base reporting a large number of SF values in a sufficiently extended range of the independent variables could be available, the function:

$$SF = SF(T_r, \dot{m}, \dot{q}, \dot{x}, d) \tag{10}$$

could be directly drawn from the data using the same MLFN heuristic procedure formerly presented for heat transfer coefficient. The knowledge of the functional form of Eq. (10) allows to determine the precise set of values of the independent variables in order to reproduce at will a selected fluid dynamics condition. This means that a control of the flow condition is obtained in practice, nevertheless avoiding at all the knowledge of the local physical phenomena. Vice versa, given the values of the controlling variables the corresponding flow condition can be identified.

As for the former heat transfer study also in this case the modeling technique here proposed totally relies on experimental data and gives then raise to a fluid specific SF function for reasons analogous to those discussed for the former α modeling [7]. In fact the fluid dynamics behavior during flow boiling at saturated conditions of a fluid is strictly linked with the present values of its thermodynamic and transport properties, which are evidently fluid specific functions controlled by the reduced temperature T_r.

For flow boiling the systematic collection and publication of precise flow pattern observations presents an even worse situation than that outlined in the preceding for heat transfer coefficients and in fact very rare sources are accessible.

For our study only the source of Schmidt [11] for the fluid R12 was usable. In this case all the measurements were taken at a single inside diameter value, preventing the assumption of d as independent variable, Eq. (10), and a SF scale corresponding to that of Fig. 3 was chosen. An MLFN function representing SF in the functional form:

$$SF = SF(T_r, \dot{m}, \dot{q}, \dot{x}) \tag{11}$$

was obtained through a procedure quite similar to the former one for α, both in the preceding of this work and in the former paper of Ref. [7], except for the substitution of the α variable with the SF one. For the 695 points of the cited source the training results are reported in Table 5 where the statistical indexes are evaluated as:

$$\begin{aligned}(\Delta)_i &= SF_i^{\text{calc}} - SF_i^{\text{exp}}\\ AAD &= \frac{1}{NPT}\sum_{i=1}^{NPT}|\Delta|_i\\ Bias &= \frac{1}{NPT}\sum_{i=1}^{NPT}(\Delta)_i\end{aligned} \tag{12}$$

In Table 7 the parameters of the obtained SF MLFN equation are also reported together with some generated data for code validation.

The obtained results, with low residual error deviations and practically without systematic shift, are very encouraging because several difficulties were notwithstanding present in the regression as the uneven distribution of the points inside the range, the rather questionable accuracy of the experimental SF

Table 5
SF MLFN equation results for the R12 data

Ref.	*NPT*	Flow	Ranges					*d* [mm]	*AAD*	*Bias*
			T_r	$\dot{m}$ [kg m^{-2} s^{-1}]	$\dot{q}$ [W m^{-2}]	$\dot{x}$	*SF*			
[11]	695	Total	0.65–0.76	0.5–578	11–80200	0.01–0.84	0.5–7.7	14	0.390	0.0005

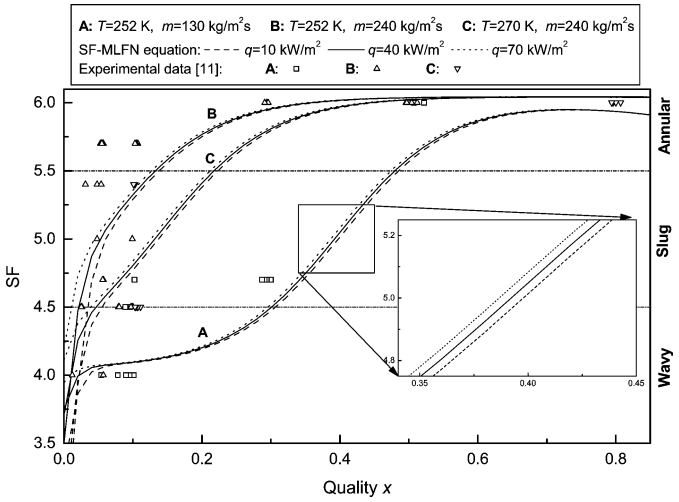

Fig. 5. Sections of the SF surface for the fluid R12 as obtained from the SF MLFN equation, Eq. (11), for three temperature T and mass rate $\dot{m}$ couples, and parametric in the heat flux $\dot{q}$.

observations, and the lack of independent sources for comparison. In fact the AAD is quite good and the equation is perfectly centered with respect to the data as the bias value assures; these results are then considered to be very promising for this totally innovative modeling method.

It is worth noting that the method does not require any further experimental work with respect to the usual one, i.e., the measurement of α with the registration of the independent variables values. Only the contextual evaluation of SF from the flow observation has to be added together with the numerical conversion according to a conventionally defined scale. Anyway, it is current practice to observe the flow condition during α measurements.

Some sections of the former SF MLFN equation for R12 are plotted in Fig. 5 where, at parametric values of the heat flux $\dot{q}$, two among the four independent variables, i.e., the temperature T and the mass rate $\dot{m}$, are fixed at three couples of values. The vapor quality range is limited to 0.84 because no data were available for higher values.

The SF scale is subdivided into the three ranges including the wavy, slug and annular flow conditions, as discussed in the preceding. At each couple of values of temperature and mass rate and for a selected value of heat flux the curve crosses the SF boundary lines delimiting the flow conditions showing the flow-dynamic evolution as a function of the vapor quality, that is at progressive sections along the tube. It is evident the smoothness of the SF surface and its weak dependence on heat flux for the flow pattern regions interested by the present temperature and mass rate values, as it is also highlighted in the enlarged section. Once a mass rate and a temperature are assigned it is possible to follow the flow condition evolution going along the corresponding line in the diagram which in fact moves through different flow regions. As the line crosses the border between two contiguous regions it also determines the vapor quality value bounding the switching from one to the other.

Following for instance one of the B lines one can see that the wavy region is passed through very quickly within a narrow $\dot{x}$ range, while the next slug region is crossed in a larger interval with a lower slope of the curve. The annular region is characterized by a very low slope and then by a large $\dot{x}$ range. At the right end of the diagram the data are lacking so it is not possible to get a reliable representation of the curves trend for $\dot{x}$ higher than 0.84.

With the decrease of the mass rate $\dot{m}$ at the same temperature T, see curves A and B, the $\dot{x}$ ranges of both the wavy and the slug flows significatively increase demonstrating that the flow pattern evolution is much more gradual with a lower $\dot{m}$. Another interesting aspect is the temperature dependence of the flow pattern evolution at a fixed mass rate $\dot{m}$ as for the curves B and C: a higher temperature T causes a slower flow pattern change in particular between the slug and annular flows.

Moreover, the flow pattern dependence on the heat flux $\dot{q}$ at annular conditions with high vapor quality, as for instance discussed in Refs. [10,16,17], cannot be verified in the present situation because of the lack of suitable experimental observations in the present literature source [11]. Where a flow condition would be observed presenting, after an annular regime, a breakup of the liquid film at the top of the internal surface of the tube as a partial dryout, the SF representation should be updated with respect to the flow evolution proposed at the Figs. 2 and 3. In this case it is suggested to introduce a new SF integer number after the annular one, $SF = 6$, indicating this partial dryout condition with $SF = 7$ and moving the mist condition to $SF = 8$. In this way the SF surface could be again represented with a continuous trend making easier its heuristic representation. Similarly, any further or even much detailed observation can be integrated at will in the present modeling method.

The asymptotic behavior of all the plotted curves when reaching higher values of quality $\dot{x}$ cannot be supported for the reduced amount of experimental observations in that region making the SF MLFN functions less reliable. The diagram of Fig. 5 reports also some points of experimental observation which show a rather evident scattering of the points themselves. The production of new data of high accuracy and reliability, also validated by different experimental sources, could render a high precision analytical representation of the flow pattern of a target fluid for flow boiling inside horizontal tubes.

After the development of the proposed heuristic flow pattern modeling technique a comparison can be set up with the more recent flow pattern model from the literature, the Thome et al. one [10,16,17]. This model is composed of a set of equations representing the boundaries between the different flow conditions having the general functional form:

$$\dot{m}_b = \dot{m}_b(T_r, \dot{m}, \dot{q}, \dot{x}, d) \tag{13}$$

in which $\dot{m}_b$ is the mass flow rate at a transition condition and $\dot{m}$ is the operative mass flow rate. The comparison between the actual value of $\dot{m}$ and the $\dot{m}_b$ calculated for each transition condition locates the present flow condition. In order to allow a comparison between the new SF MLFN surface and the model it is necessary to generate from the new SF MLFN equation the analogous boundary curves of that model. From a numer-

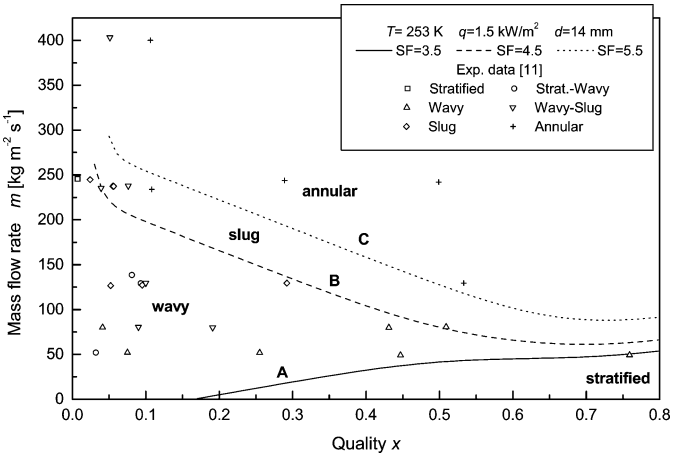

Fig. 6. Contours lines of the SF surface for the fluid R12 as obtained from the SF MLFN equation, Eq. (11), for the typical flow conditions boundaries. Experimental observations from Ref. [11].

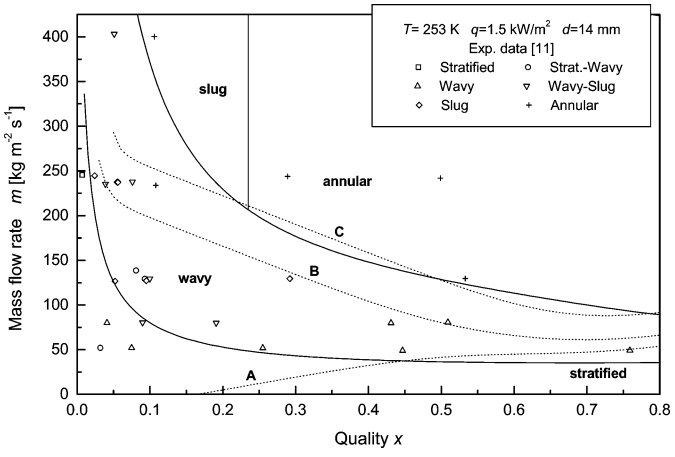

Fig. 7. Contours lines for the fluid R12 as obtained from the SF MLFN surface, Eq. (11), and from the Thome et al. flow pattern model [10] for the typical flow conditions boundaries. Experimental observations from Ref. [11].

ical inversion of the SF MLFN surface, Eq. (10), one gets the equivalent form:

$$\dot{m} = \dot{m}(SF, T_r, \dot{q}, \dot{x}, d) \tag{14}$$

and assigning to it constants value of SF, as for instance $SF = 4.5$ in between wavy and slug flow conditions, and $SF = 5.5$ in between slug and annular ones, the boundary lines from the SF MLFN equation with a format corresponding to that of the Thome et al. model are obtained.

In Fig. 6 such a representation is plotted in the same coordinates mass rate $\dot{m}$ and vapor quality $\dot{x}$ assumed by Thome et al. [10,16,17] in their flow pattern models, for assigned values of the temperature T and heat flux $\dot{q}$. Four flow conditions, from stratified to annular, are shown together with the boundary lines between them, lines A, B, and C. Always considering the not favourable data situation it can be for instance pointed out that the stratified-wavy boundary line should be decreasing monotonic instead of increasing monotonic as in the plot. In fact at a given mass rate the increase of vapor quality along the tube would change the flow condition from stratified to wavy and not vice versa as represented in the plot. This is considered an inconsistency due to the unsuitable data base, but not to the modeling technique. Once more the data have the leading role for an accurate modeling in heat transfer and therefore the data are required with the best uncertainty as possible.

The comparison between the SF MLFN boundary lines and those from the Thome et al. model are presented in Fig. 7. The contours lines for the typical flow conditions boundaries, as obtained from the cited model, have been reported with continuous lines. The boundary lines delimit the labeled flow condition regions according to the model. The present slug condition is corresponding to the intermittent one in the Thome et al. terminology. On the same diagram the corresponding boundary lines from the present SF MLFN surface are also plotted with dashed lines for comparison and labeled again with the A, B, and C letters, together with the experimental observations from Ref. [11]. The flow condition regions according to the SF MLFN subdivision are deduced from the former Fig. 6.

From an analysis of the plots of Fig. 7 a general correspondence between the two methods of delimitation of the flow condition regions can be ascertained. The boundaries between stratified and wavy regions could agree each other in the case the line A could be modified from a line increasing with vapor quality to something like a horizontal line, as already pointed out. The boundary between wavy and annular regions also looks to be consistent with the corresponding line C. The slug (intermittent) region is the really incoherent one: for the Thome model it lies below a constant vapor quality value and it is located at higher mass rates. Consequently, at lower mass rates a direct transition from wavy to annular flow is shown and this is rather difficult to understand. The limited number of experimental observations that it was possible to report into the graph gives interlocutory results for both the methods.

The numerical results of the flow pattern subdivision according to the two methods are reported in Table 6. The data from Ref. [11] are grouped as from the experimental observations in four subsets of flow regime. For each of these subsets the present SF MLFN and the Thome map have been applied finding the number of points falling inside the same condition according to the single model; these numbers are indicated with bold characters. The points classified as falling in other flow regimes are reported as well. The points falling exactly on the boundary lines are omitted from this analysis. The present SF MLFN map correctly identifies all the bubbly and plug points, the 89% of the stratified + wavy points and the 82% of the annular + mist ones, but it takes roughly only half of the slug points. For the present map the correspondence for the various conditions between the predictions and the experimental observations looks to be quite good, also considering the evident limits of the accuracy of the experimental source.

On the other hand the Thome et al. model tends to concentrate the bubbly + plug, the stratified + wavy, and the slug points into the stratified + wavy condition. The annular condition is recognized only for the 41% of the points.

This limited comparison between the two methods looks then to be largely favourable to the present SF MLFN map.

Table 6
Comparison of the present SF map and of the Thome flow pattern map [10] with the experimental flow subdivision for R12

Experimental flow subdivision			Present SF MLFN map								Thome flow pattern map [10]							
Ref.	Flow regime	*NPT*	Bubbly + Plug		Stratified + Wavy		Slug		Annular + Mist		Bubbly + Plug		Stratified + Wavy		Slug		Annular + Mist	
			NPT	%	*NPT*	%	*NPT*	%	*NPT*	%	*NPT*	%	*NPT*	%	*NPT*	%	*NPT*	%
[11]	Bubbly + Plug	16	**16**	**100.0**	–	–	–	–	–	–	–	–	16	100.0	–	–	–	–
[11]	Stratified + Wavy	239	–	–	**213**	**89.1**	26	10.9	–	–	–	–	**239**	**100.0**	–	–	–	–
[11]	Slug	111	–	–	54	48.6	**51**	**46.0**	6	5.4	–	–	111	100.0	–	–	–	–
[11]	Annular + Mist	213	–	–	–	–	39	18.3	**174**	**81.7**	–	–	45	21.2	80	37.5	**88**	**41.3**

Table 7
Parameters of the SF MLFN equation for the fluid R12

SF MLFN parameters for R12					
I	5	γ	1	$A_{\max}$	0.95
J	3	β	0.005	Bias 1	1
K	1	$A_{\min}$	0.05	Bias 2	1
$V_{\min,1} \equiv T_r^{\min}$	0.5	$V_{\min,3} \equiv \dot{q}^{\min}$	0	$W_{\min,1} \equiv SF^{\min}$	0
$V_{\max,1} \equiv T_r^{\max}$	1.0	$V_{\max,3} \equiv \dot{q}^{\max}$	120000	$W_{\max,1} \equiv SF^{\max}$	8
$V_{\min,2} \equiv \dot{m}^{\min}$	0	$V_{\min,4} \equiv \dot{x}^{\min}$	0		
$V_{\max,2} \equiv \dot{m}^{\max}$	1500	$V_{\max,4} \equiv \dot{x}^{\max}$	1		

i	j	w_{ij}	i	j	w_{ij}
1	1	−1531.10411	1	3	−1243.11569
2	1	6535.33489	2	3	6415.40398
3	1	−5.99054691	3	3	30.3882699
4	1	−633.008885	4	3	1368.62115
5	1	770.769501	5	3	−994.686023
1	2	−1053.89585	j	k	w_{jk}
2	2	2599.76697	1	1	2545.25166
3	2	−467.745879	2	1	−154.129081
4	2	−8462.44137	3	1	97.2598862
5	2	369.587433	4	1	−2543.01221

Data generated for code validation				
T_r	$\dot{m}$	$\dot{q}$	$\dot{x}$	SF
0.66	100	1500	0.3	4.16
0.66	200	10000	0.7	6.04
0.71	200	20000	0.4	5.66
0.71	150	15000	0.6	5.74

Apart from the former analysis the value of present results cannot be considered as definitive because the data base on which this study has been developed is too much limited. The present work is intended most of all as a proposal of a new modeling procedure rather than a set of conclusive results.

7. Local heat transfer and flow pattern modeling

Both in the former [7] and in the present studies it has been demonstrated that for flow boiling inside a horizontal tube the heat transfer coefficient can be heuristically represented as a function of only the physical controlling variables which reads:

$$\alpha = \alpha(T_r, \dot{m}, \dot{q}, \dot{x}, d) \tag{7}$$

and this function is fluid dependent and relies only on experimental data regularly distributed in the range of interest. This formulation was shown to be able to represent in total the heat transfer surface for all the possible flow conditions encountered along the tube. Heat transfer subdivisions into subsets according to homogeneous flow conditions can be represented as well with similar accuracies.

At the same time, it has been shown here that the flow condition evolution during the flow boiling inside a tube can be represented through the introduction of the *SF* (Strömungform = form of the flow) conventional variable and heuristically developing the corresponding function in the physical controlling variables:

$$SF = SF(T_r, \dot{m}, \dot{q}, \dot{x}, d) \tag{10}$$

Also this function can represent at once all the flow conditions along the tube.

Recent studies in the literature tend to recognize that the heat transfer representation has to be built from a number of local heat transfer representations each one specialized for a particular homogeneous flow condition. The delimitation of these homogeneous flow conditions necessarily requires a flow pattern model to identify the subranges of the physical controlling

variables corresponding to each flow condition. A number of specialized heat transfer equations are then linked with a flow pattern model making then the heat transfer representation to be flow pattern dependent. This is in fact the case of the Thome et al. model [2,10].

In this context it cannot be stated that a flow boiling heat transfer model has in general to be flow pattern dependent because such a situation is merely the consequence of the assumed modeling framework and not an intrinsic fundamental necessity. In fact in the heat transfer modeling method proposed in the former work [7] no element of a flow condition representation, neither from the present SF MLFN method nor from any conventional flow pattern model, enters the global MLFN heat transfer coefficient representation across all the flow conditions.

On the other hand, proceeding only through mathematical formalism one could demonstrate that a heat transfer model cannot be dependent on a flow pattern functional representation. In fact moving from the former heuristic heat transfer model, Eq. (7), in the case of a flow pattern dependence that equation would be modified reading:

$$\alpha = \alpha(SF, T_r, \dot{m}, \dot{q}, \dot{x}, d) \tag{15}$$

and since SF is a function of the same physical variables $(T_r, \dot{m}, \dot{q}, \dot{x}, d)$, Eq. (10), it is also:

$$\alpha = \alpha\big[SF(T_r, \dot{m}, \dot{q}, \dot{x}, d), T_r, \dot{m}, \dot{q}, \dot{x}, d\big] \tag{16}$$

which turns SF to become a redundant variable in Eq. (16). It can then be concluded that both the heat transfer and the flow pattern analytical representations are independent each other, even if they share the same set of independent physical variables.

The two physical phenomena, the heat transfer and the fluid dynamics behavior, are clearly connected in parallel for their physical evolutions, but they can be maintained independent for their functional representations.

8. Conclusions

After a former work [7] dealing with the heuristic representation of the heat transfer coefficient during flow boiling inside horizontal tubes, in the present paper the same modeling technique based on neural networks as a universal function approximator is applied to study the local representation of flow boiling heat transfer at varying fluid dynamics conditions along the tube, i.e., moving through different flow pattern regions. After the subdivision of the experimental data into subsets homogeneous for a defined range of flow conditions specific heat transfer equations have been heuristically got. Such a subdivision has been performed either according to the experimental observation, where available, or, alternatively, by a conventional flow pattern model. These specific equations have been validated and compared with the global MLFN heat transfer coefficient representation for the same target fluid. This study has been extended to four fluids for which suitable data were available from the literature.

The study showed that the representation capabilities of these specialized models are very high, probably with a potentiality exceeding the current experimental uncertainty, and they always slightly overcame the corresponding global MLFN heat transfer coefficient equation. This is likely due to the greater ease in approximating a reduced extent of heat transfer surface instead of representing the whole surface. The small increase of accuracy obtained does not suggest to adopt such method in general because it results to be more complicated for both the equations development and for the equations practical use. This has also indirectly shown that a high accuracy flow boiling heat transfer equation can be developed without any relation with local fluid dynamics conditions.

Further on, a new modeling technique has been proposed for the fluid dynamics conditions along the tube. According to this new idea the actual picture of the flow condition, as observed by an experimenter during the registration of a heat transfer value, is directly linked with a conventional real number ranging in a standardized interval, the so-called SF factor. The comparison of a present flow condition picture, as observed by the experimenter, with the pre-established sequence of flow conditions images related to the SF scale allows to convert the actual flow condition into a conventional numerical value. Such a link establishes then a biunique relationship. The conventional SF flow condition value of experimental origin can be therefore converted into a continuous fluid specific function through a MLFN technique similar to that already applied for the heat transfer coefficient.

Proceeding through this new modeling method for the flow condition, the only available literature data reporting SF values have been processed producing the corresponding SF MLFN equation for the full range of flow conditions. This function has also been converted into a format similar to that assumed by the more recent literature flow pattern models in order to compare the respective contours. The method proved to have a quite good performance and coherence in representing the whole SF surface at the only condition that data are evenly presented inside the interest range of variables. The present SF MLFN equation and the more recent literature flow pattern model demonstrated to get comparable results, in spite of the limited data base.

The proposed method is considered as promising and straightforward for the modeling purpose, but the formation of a systematic data base through the publication of SF data is absolutely needed to consolidate the method and to allow a reliable application of such heuristic technique.

Finally, this study has also shown that in general a flow boiling heat transfer model is not flow pattern dependent because no element of a flow condition representation is required to enter the global MLFN heat transfer coefficient modeling valid across all the flow conditions.

References

[1] N. Kattan, J.R. Thome, D. Favrat, Flow boiling in horizontal tubes, Part 3: Development of a new heat transfer model based on flow patterns, J. Heat Transfer 120 (1) (1998) 156–165.

[2] J.R. Thome, On recent advances in modeling of two-phase flow and heat transfer, Heat Transfer Engrg. 24 (6) (2003) 46–59.

[3] J.R. Thome, J. El Hajal, Flow boiling heat transfer to carbon dioxide: general prediction method, Int. J. Refrig. 27 (2004) 294–301.

[4] R. Span, Multiparameter Equations of State, Springer, Berlin, 2000.

[5] G. Cristofoli, L. Piazza, G. Scalabrin, A viscosity equation of state for R134a through a multi-layer feedforward neural network technique, Fluid Phase Equilibria 199 (2002) 223–236.

[6] G. Scalabrin, G. Cristofoli, The viscosity surfaces of propane in the form of multilayer feed forward neural networks, Int. J. Thermophys. 24 (5) (2003) 1241–1263.

[7] G. Scalabrin, M. Condosta, P. Marchi, Modeling flow boiling heat transfer of pure fluids through artificial neural networks, Int. J. Therm. Sci. 45 (7) (2006) 643–663.

[8] G. Scalabrin, L. Piazza, Analysis of forced convection heat transfer to supercritical carbon dioxide inside tubes using neural networks, Int. J. Heat Mass Transfer 46 (2003) 1139–1154.

[9] G. Scalabrin, L. Piazza, M. Condosta, Convective cooling of supercritical carbon dioxide inside tubes: heat transfer analysis through neural networks, Int. J. Heat Mass Transfer 46 (2003) 4413–4425.

[10] J.R. Thome, J. El Hajal, Two-phase flow pattern map for evaporation in horizontal tubes: latest version, Heat Transfer Eng. 24 (6) (2003) 3–10.

[11] H. Schmidt, Beitrag zum Verständnis des Wärmeübergangs im horizontalen Verdampferrohr, in: Fortschr.-Ber. VDI, Reihe 19, vol. 6, VDI-Verlag, Düsseldorf, 1986.

[12] J.M. Chawla, Wärmeübergang und Druckabfall in waagerechten Rohren bei der Strömung von verdampfenden Kältemitteln, in: VDI-Forschungsheft, vol. 523, VDI-Verlag, Düsseldorf, 1967.

[13] J.Y. Shin, M.S. Kim, S.T. Ro, Experimental study on forced convective boiling heat transfer of pure refrigerants and refrigerant mixtures in a horizontal tube, Int. J. Refrig. 20 (1997) 267–275.

[14] M. Lallemand, C. Branescu, P. Haberschill, Local heat transfer coefficients during boiling of R22 and R407C in horizontal smooth and microfin tubes, Int. J. Refrig. 24 (2001) 57–72.

[15] T.Y. Choi, Y.J. Kim, M.S. Kim, S.T. Ro, Evaporation heat transfer of R-32, R-134a, R-32/134a, and R-32/125/134a inside a horizontal smooth tube, Int. J. Heat Mass Transfer 43 (2000) 3651–3660.

[16] N. Kattan, J.R. Thome, D. Favrat, Flow boiling in horizontal tubes, Part 1: Development of a diabatic two-phase flow pattern map, J. Heat Transfer 120 (1) (1998) 140–147.

[17] O. Zürcher, D. Favrat, J.R. Thome, Development of a diabatic two-phase flow pattern map for horizontal flow boiling, Int. J. Heat Mass Transfer 45 (2002) 291–301.